TÜBİTAK

Turkish Journal of Engineering & Environmental Sciences

http://journals.tubitak.gov.tr/engineering/

Research Article

Turkish J Eng Env Sci
(2013) 37: 1 – 15

doi:10.3906/muh-1201-17

Small scale effect on electro-thermo-mechanical vibration analysis of single-walled boron nitride nanorods under electric excitation

Mehdi MOHAMMADIMEHR[1,*], **Amir Hossein RAHMATI**[1]
[1]Department of Mechanical Engineering, Faculty of Engineering, University of Kashan, Kashan, Iran

Received: 30.01.2012 • **Accepted:** 05.07.2012 • **Published Online:** 04.03.2013 • **Printed:** 01.04.2013

Abstract: In this article, electro-thermo-nonlocal axial vibration analysis of single-walled boron nitride nanorods (SWBNNRs) under electric excitation is investigated. A constitutive equation for the nanorods under electro-thermo-mechanical loadings is obtained using the small scale effect. The effects of the small scale, aspect ratio, and clamped–clamped (C–C) and clamped–free (C–F) boundary conditions on the natural frequency are discussed. The effects of the dielectric constant, piezoelectric coefficient, electric excitation, 2 boundary conditions, and temperature change on the axial displacement of SWBNNRs are investigated. The results show that the natural frequency decreases with increasing small scale effect. The axial displacement of SWBNNRs increases with an increase in the temperature change and also, for the piezoelectric coefficient, it is the same. The results of this research can be used for micro- and nano-electro-thermo-mechanical devices and nanoelectronics.

Key words: Single-walled boron nitride nanorods, electro-thermo-mechanical loadings, axial vibration, electric excitation, nonlocal elasticity theory

1. Introduction

Carbon nanotubes (CNTs) were discovered by Iijima (1991). These materials had uniform electronic structures and high thermal and strength properties so that their electrical properties were not stable. However, in contrast to CNTs, boron nitride nanotubes (BNNTs) had stable semiconducting behavior with a large band gap (Bansal et al., 2006).

Several studies (Yoon et al., 2003; He et al., 2005; Fu et al., 2006; Aydoğdu and Ece, 2007) investigated the buckling or/and vibration of CNTs using the local continuum theory. This theory states that the stress state at a reference point in the body is only dependent on the strain state at this point.

In other studies, it has been shown that the small scale effect has a significant role in the analysis of CNTs and BNNTs and should be included in the formulations. The nonlocal elasticity theory was first introduced by Eringen (1983). He stated that the stress state at a reference point in the body was regarded as dependent not only on the strain state at this point but also on the strain states at all of the points throughout the body. Salehi-Khojin and Jalili (2008) presented the buckling of BNNTs reinforced piezoelectric polymeric composites under combined electro-thermo-mechanical loadings. Their results showed that the piezoelectric matrix increases the buckling resistance of the composite substantially, and the supporting effect of elastic medium depends on the direction of applied voltage and thermal flow. Aydogdu (2009) considered the small scale effect on

*Correspondence: mmohammadimehr@kashanu.ac.ir

axial vibration of nanorods and also explicit formulations derived for natural frequencies for clamped–clamped (C–C) and clamped–free (C–F) boundary conditions. Ghorbanpour Arani et al. (2010) studied the transverse vibrations of single-walled carbon nanotubes (SWCNTs) and double-walled carbon nanotubes (DWCNTs) under axial loading by applying the Euler–Bernoulli and Timoshenko beam models and the Donnell shell model. They concluded that the Euler–Bernoulli beam model and the Donnell shell model predictions have the lowest and highest accuracies, respectively. In order to predict the vibration behavior of the CNT more accurately, the classical models were modified using the nonlocal theory. Moreover, they obtained the natural frequencies and amplitude coefficient for the simply supported (S-S) boundary conditions. Mohammadimehr et al. (2010a) investigated the small scale effect on the torsional buckling of a DWCNT embedded on Winkler and Pasternak foundations. They considered the effects of the surrounding elastic medium, such as the spring constant of the Winkler type and the shear constant of the Pasternak type, as well as the van der Waals (vdW) forces between the inner and outer nanotubes. They showed that the shear constant of the Pasternak type increases the nonlocal critical torsional buckling load, while the difference between the presence and absence of the shear constant of the Pasternak type was large. Furthermore, they concluded that the nonlocal critical buckling load is lower than the local critical buckling load. Using the nonlocal elasticity theory, Ghorbanpour Arani et al. (2011) presented the thermal effect on the buckling analysis of a DWCNT embedded in an elastic medium based on Pasternak foundation subjected to a uniform external pressure. They indicated that the effect of temperature change on the critical buckling pressure is negligible, especially for a stiff elastic medium; however, this is not the case if the elastic medium is soft. Ghorbanpour Arani et al. (2012a) illustrated the buckling analysis of double-walled boron-nitride nanotubes (DWBNNTs) surrounded by a bundle of CNTs subjected to electro-thermo-mechanical loadings, using an energy method based on the Winkler–Pasternak model and nonlocal piezoelasticity cylindrical shell theory. They considered the effects of electric and thermal fields, elastic medium, and small scale parameter on the electro-thermo-mechanical buckling behavior of DWBNNTs.

Aydogdu (2012) studied the nonlocal axial vibration of SWCNTs embedded in an elastic medium. He investigated the effect of various parameters like stiffness of elastic medium, C–C and C–F boundary conditions, and nonlocal parameters on the axial vibration of nanorods. Ghorbanpour Arani et al. (2012b) presented the electro-thermo-nonlocal transverse vibration behavior of DWBNNTs embedded in an elastic medium using nonlocal piezoelasticity cylindrical shell theory. They investigated the effects of the spring constant of Winkler-type, shear constant of Pasternak-type, electric field, and temperature change on the dimensionless natural frequency. They concluded that the influence of electric field on the dimensionless natural frequency is approximately constant, while it decreases with increasing temperature change.

The aim of this research was to study electro-thermo-nonlocal axial vibration analysis of SWBNNRs under electric excitation. The influences of the dielectric constant, piezoelectric coefficient, electric excitation, C–C and C–F boundary conditions, and temperature change on the axial displacement of SWBNNRs are considered.

2. Nonlocal rod model

The nonlocal elasticity model was first presented by Eringen (1983). According to this model, the stress at a reference point in the body is dependent not only on the strain state at that point, but also on the strain state at all of the points throughout the body. The constitutive equation of the nonlocal elasticity can be written as follows (Eringen, 1983):

$$[1-(e_0a)^2\nabla^2]\sigma_{ij} = C_{ijkl}\,\varepsilon_{kl} - e_{ijk}E_k, \tag{1}$$

where e_0 denotes a constant. e_0a is the nonlocal parameter showing the small scale effect. This parameter was determined by matching the dispersion curves based on the atomic models (Eringen, 1983).

Total strain second-order tensor is considered as

$$\varepsilon_{kl} = \varepsilon_{kl}^{M} + \varepsilon_{kl}^{T}, \tag{2}$$

where ε_{kl}^{M} and ε_{kl}^{T} are the mechanical and thermal strains respectively.

Figure 1 illustrates the nanorods under electro-thermo-mechanical loadings and electric excitation. This figure shows a SWBNNR of length L, thickness h_0, and diameter d.

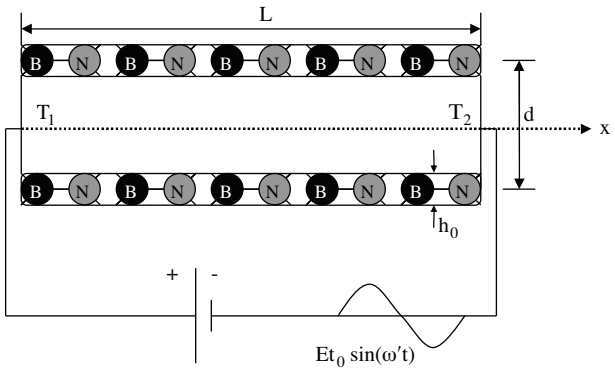

Figure 1. A schematic view of a SWBNNR under electro-thermo-mechanical loadings and electric excitation.

According to Figure 1, for axial vibration of thin nanorods under electro-thermal loadings, Eq. (1) can be expressed as follows (Aydogdu, 2009):

$$[1-(e_0a)^2\frac{d^2}{dx^2}]\sigma_x = E\varepsilon_x - h\,E_x - \alpha_x\,E\,T(x) \tag{3}$$

The axial strain in terms of axial displacement is defined as

$$\varepsilon_x = \frac{\partial u(x,t)}{\partial x} \tag{4}$$

3. Heat conduction equation

For the steady state, the heat conduction equation without any heat source is considered as the following form (Shodja and Ghahremaninejad, 2006):

$$\nabla.(k\nabla T) = 0 \tag{5}$$

where k is the constant thermal conduction coefficient.

Using Eq. (5), the heat conduction equation of the nanorods can be written in the following one-dimensional form:

$$\frac{d^2T}{dx^2} = 0 \tag{6}$$

The solution of Eq. (6) is obtained as follows:

$$T(x) = c_1x + c_2, \tag{7}$$

where c_1 and c_2 are real constants. These constants are obtained by boundary conditions, which are considered as follows:

$$T(x=0)=T_1, T(x=L)=T_2 \tag{8}$$

Substituting Eq. (7) into Eq. (8) yields

$$T(x)=\frac{T_2-T_1}{L}x+T_1 \tag{9}$$

4. Maxwell's equation

The electric displacement can be written as

$$D=h\varepsilon_x+\eta E_x-pT(x), \tag{10}$$

where η and p are the dielectric constant and pyroelectric coefficient, respectively.

Maxwell's equation for the free electric charge density is defined as (Khoshgoftar et al., 2009)

$$\nabla .D=0 \tag{11}$$

Eq. (11) is obtained in the following one-dimensional form:

$$\frac{dD}{dx}=0 \tag{12}$$

Substituting Eq. (10) into Eq. (12) yields

$$\frac{dE_x}{dx}=\frac{p}{\eta}\frac{dT(x)}{dx}-\frac{h}{\eta}\frac{d\varepsilon_x}{dx} \tag{13}$$

Variation in electric field by substituting Eqs. (4) and (9) into Eq. (13) is given by

$$\frac{dE_x}{dx}=\frac{T_2-T_1}{L}\frac{p}{\eta}-\frac{h}{\eta}\frac{\partial^2 u(x,t)}{\partial x^2} \tag{14}$$

5. The free vibration of the nanorods

The axial force per unit length is defined as

$$N_x=\int \sigma_x\, dA \tag{15}$$

Substituting Eq. (3) into Eq. (15) yields

$$[1-(e_0a)^2\frac{d^2}{dx^2}]N_x=AE\varepsilon_x-Ah\,E_x-\alpha_x A\,E\,T(x) \tag{16}$$

The equation of motion for the electro-thermo-axial vibration of the SWBNNRs can be obtained as

$$\frac{\partial N_x}{\partial x}=m\frac{\partial^2 u(x,t)}{\partial t^2} \tag{17}$$

Using Eqs. (4), (9), and (14), substituting Eq. (16) into Eq. (17) yields the following equation of motion for SWBNNRs:

$$[1-(e_0a)^2\frac{d^2}{dx^2}]m\frac{\partial^2u}{\partial t^2}=A(E+\frac{h^2}{\eta})\frac{\partial^2u}{\partial x^2}-A\frac{T_2-T_1}{L}(\frac{hp}{\eta}+\alpha_xE) \tag{18}$$

Using separation, $u(x,t)$ can be defined as

$$u(x,t)=F(x)\sin(\omega t) \tag{19}$$

To obtain natural frequency, the homogeneous part of Eq. (18) is considered as follows:

$$[1-(e_0a)^2\frac{d^2}{dx^2}]m\frac{\partial^2u}{\partial t^2}=A(E+\frac{h^2}{\eta})\frac{\partial^2u}{\partial x^2} \tag{20a}$$

Substituting Eq. (19) into Eq. (20a) yields

$$\frac{d^2F}{dx^2}+\beta^2F=0, \tag{20b}$$

where

$$\beta^2=\frac{\Omega^2}{1-(e_0a)^2\Omega^2}, \tag{21a}$$

$$\Omega^2=\frac{m\omega^2}{EA+\frac{h^2A}{\eta}} \tag{21b}$$

It is important to note that the effect of temperature change is entered in the nonhomogeneous part of Eq. (18); thus it has no effect on the natural frequency (according to Eqs. (20a) and (21b))

The solution of above equation can be written as

$$F(x)=A_1\cos(\beta x)+B_1\sin(\beta x), \tag{22}$$

where A_1 and B_1 are real constants. These constants are obtained using 2 different boundary conditions defined as follows:

$$\begin{aligned}&u(0,t)=u(L,t)=0 \quad C-C \text{ boundary condition}\\&u(0,t)=N_x(L,t)=0 \quad C-F \text{ boundary condition}\end{aligned} \tag{23}$$

5.1. The natural frequency of nanorods under the C–C supported case

For the C–C supported case, substituting Eqs. (19) and (22) into Eq. (23) yields

$$\begin{aligned}&A_1=0,\\&\sin(\beta l)=0\,,\end{aligned} \tag{24}$$

where

$$\beta=\frac{i\,\pi}{L},\ i=1,2,...,n \tag{25}$$

Using Eqs. (21a), (21b), and (25), the natural frequency of nanorods for the C–C supported case is obtained as

$$\omega^2=\frac{(\frac{i\,\pi}{L})^2\,(E\,A+\frac{h^2}{\eta}A)}{m\left[1+(e_0a)^2(\frac{i\,\pi}{L})^2\right]},\ i=1,2,...,n \tag{26}$$

5.2. The natural frequency of nanorods under the C–F supported case

Using Eqs. (19) and (22), β for the C–F supported case is written as

$$\beta = \frac{(2i-1)\,\pi}{2L},\ i = 1, 2, ..., n \tag{27}$$

For the C–F supported case, the natural frequency of nanorods using Eqs. (21a), (21b), and (27) is considered as follows:

$$\omega^2 = \frac{(\frac{(2i-1)\,\pi}{2L})^2\,(E\,A + \frac{h^2}{\eta}A)}{m\left[1 + (e_0 a)^2(\frac{(2i-1)\,\pi}{2L})^2\right]},\ i = 1, 2, ..., n \tag{28}$$

6. The forced vibration of the SWBNNRs under electro-thermo-mechanical loadings

The forced vibration of the SWBNNRs under electro-thermo-mechanical loadings for the electric excitation can be written as

$$[1 - (e_0 a)^2 \frac{d^2}{dx^2}]m\frac{\partial^2 u}{\partial t^2} = A(E + \frac{h^2}{\eta})\frac{\partial^2 u}{\partial x^2} - A\frac{T_2 - T_1}{L}(\frac{hp}{\eta} + E\alpha_x) + E_0 \sin(\omega' t), \tag{29}$$

where E_0 and ω' are the amplitude and frequency of electric excitation, respectively.

The axial displacement of the SWBNNRs is obtained using the C–C and C–F boundary conditions.

6.1. The axial displacement of the SWBNNRs for the C–C supported case

Using separation, $u(x,t)$ for the C–C supported case (Eq. (23)) can be obtained as

$$\begin{aligned} &u(x,t) = [F_i(x)]^T_{n\times 1}\,[G_i(t)]_{n\times 1} \\ &F_i(x) = \sin(\tfrac{i\pi x}{L}), i = 1, 2, ..., n \end{aligned} \tag{30}$$

Substituting Eq. (30) into Eq. (29), the governing equation of motion for the SWBNNRs is expressed as

$$\begin{aligned} &\sum_{i=1}^{n} m(1 + (\tfrac{i\pi}{L})^2(e_0 a)^2)\sin(\tfrac{i\pi x}{L})\ddot{G}_i(t) + \sum_{i=1}^{n}\left[(\tfrac{i\pi}{L})^2\left(EA + \tfrac{h^2 A}{\eta}\right)\sin(\tfrac{i\pi x}{L})G_i(t)\right] \\ &= k' + E_0 \sin(\omega' t)\,, i = 1, 2, ..., n, \end{aligned} \tag{31}$$

where

$$k' = -\frac{T_2 - T_1}{L}A(\frac{hp}{\eta} + E\alpha_x) \tag{32}$$

Multiplying Eq. (31) in $\sin(\frac{j\pi x}{L}), j = 1, 2, ..., n$ and then integrating in terms of nanorod length, ordinary differential equations (ODEs) are obtained. These equations have homogeneous and particular solutions that are considered as the following form:

$$G_i(t) = G_{hi}(t) + G_{pi}(t), \tag{33}$$

where $G_{hi}(t)$ and $G_{pi}(t)$ are the homogeneous and particular solutions, respectively, expressed as

$$G_{hi}(t) = C_{i1}\sin(\beta_i t) + C_{i2}\cos(\beta_i t), \tag{34}$$

$$G_{pi}(t) = C_{i3} + C_{i4}\sin(\omega' t), \tag{35}$$

where

$$\beta_i = \sqrt{\frac{\left(EA + \frac{h^2 A}{\eta}\right)(\frac{i\pi}{L})^2}{m\left[1 + (e_0 a)^2(\frac{i\pi}{L})^2\right]}}$$

Using Eqs. (31) and (35), C_{i3} and C_{i4} constants can be written as

$$C_{i3} = \frac{2k'(1-(-1)^i)}{i\pi\left(EA + \frac{h^2 A}{\eta}\right)(\frac{i\pi}{L})^2}, \tag{36}$$

$$C_{i4} = \frac{2E_0(1-(-1)^i)}{i\pi\left[\left(EA + \frac{h^2 A}{\eta}\right)(\frac{i\pi}{L})^2 - m\omega'^2(1 + (e_0 a)^2(\frac{i\pi}{L})^2)\right]}, \tag{37}$$

where C_{i1} and C_{i2} are real constants. These constants are obtained using the initial conditions, considered as

$$\begin{aligned} &G(t=0) = 0, \\ &\dot{G}(t=0) = 0 \end{aligned} \tag{38}$$

Substituting Eq. (33) into Eq. (38) yields

$$C_{i2} = -C_{i3}, \tag{39}$$

$$C_{i1} = -\frac{\omega'}{\beta_i} C_{i4} \tag{40}$$

Substituting Eqs. (34) and (35) into Eqs. (33) and (30), the axial displacement of the SWBNNRs under electro-thermo-mechanical loadings for electric excitation and C-C supported case is expressed as follows:

$$\begin{aligned} &u(x,t) = [F_i(x)]^T_{n\times 1} \times \left(\begin{array}{l} [\sin(\beta_i t)]_{n\times 1}[I]_{n\times n}[C_{i1}]_{n\times 1} \\ +[\cos(\beta_i t)]_{n\times 1}[I]_{n\times n}[C_{i2}]_{n\times 1} + \\ [C_{i3}]_{n\times 1} + [\sin(\omega' t)]_{n\times 1}[I]_{n\times n}[C_{i4}]_{n\times 1} \end{array} \right) \\ &i = 1, 2, ..., n \end{aligned} \tag{41}$$

6.2. The axial displacement of the SWBNNRs for the C–F supported case

The axial displacement of nanorods for the C–F supported case is written as

$$\begin{aligned} &u(x,t) = [F_i(x)]^T_{n\times 1}[G_i(t)]_{n\times 1} \\ &F_i(x) = \sin(\tfrac{(2i-1)\pi x}{2L}), i = 1, 2, ..., n \end{aligned} \tag{42}$$

Substituting Eq. (42) into Eq. (29) yields

$$\begin{aligned} &\sum_{i=1}^{n} m(1 + (\tfrac{(2i-1)\pi}{2L})^2(e_0 a)^2)\sin(\tfrac{(2i-1)\pi x}{2L})\ddot{G}_i(t) + \\ &\sum_{i=1}^{n}\left[(\tfrac{(2i-1)\pi}{2L})^2\left(EA + \tfrac{h^2 A}{\eta}\right)\sin(\tfrac{(2i-1)\pi x}{2L})G_i(t)\right] = k' + E_0\sin(\omega' t) \\ &, i = 1, 2, ..., n \end{aligned} \tag{43}$$

Multiplying Eq. (43) in $\sin(\frac{(2j-1)\pi x}{2L}), j = 1, 2, ..., n$ and then integrating in terms of nanorod length, ODEs are obtained. The solution of ODEs is defined as

$$G_{hi}(t) = C_{i5}\sin(\beta_i t) + C_{i6}\cos(\beta_i t), \tag{44}$$

$$G_{pi}(t) = C_{i7} + C_{i8}\sin(\omega' t), \tag{45}$$

where

$$\beta_i = \sqrt{\frac{\left(EA + \frac{h^2 A}{\eta}\right)(\frac{(2i-1)\pi}{2L})^2}{m\left[1 + (e_0 a)^2(\frac{(2i-1)\pi}{2L})^2\right]}}$$

Using Eqs. (43) and (45), C_{i7} and C_{i8} constants are expressed as follows:

$$C_{i7} = \frac{4k'}{(2i-1)\pi\left(EA + \frac{h^2 A}{\eta}\right)\left(\frac{(2i-1)\pi}{2L}\right)^2}, \tag{46}$$

$$C_{i8} = \frac{4E_0}{(2i-1)\pi\left[\left(EA + \frac{h^2 A}{\eta}\right)(\frac{(2i-1)\pi}{2L})^2 - m\omega'^2(1 + (e_0 a)^2(\frac{(2i-1)\pi}{2L})^2)\right]} \tag{47}$$

Using Eqs. (33), (38), and (44), C_{i5} and C_{i6} constants are written as

$$C_{i6} = -C_{i7}, \tag{48}$$

$$C_{i5} = -\frac{\omega'}{\beta_i}C_{i8} \tag{49}$$

The axial displacement of the SWBNNRs for the C–F supported case is obtained as follows:

$$\begin{aligned} u(x,t) &= [F_i(x)]^T_{n\times 1} \times \left(\begin{array}{l} [\sin(\beta_i t)]_{n\times 1}[I]_{n\times n}[C_{i5}]_{n\times 1} \\ +[\cos(\beta_i t)]_{n\times 1}[I]_{n\times n}[C_{i6}]_{n\times 1} + \\ [C_{i7}]_{n\times 1} + [\sin(\omega' t)]_{n\times 1}[I]_{n\times n}[C_{i8}]_{n\times 1} \end{array} \right) \\ & i = 1, 2, ..., n \end{aligned} \tag{50}$$

7. Numerical results and discussion

The nanorod's dimensions and its thermal, electrical, and mechanical properties can be considered as follows (Salehi-Khojin and Jalili, 2008; Khoshgoftar et al., 2009; Mustapha and Zhong, 2010; Mohammadimehr et al., 2010a, 2010b):

$$\begin{aligned} &E{=}5.5\,Tpa, r{=}12.306\,nm, h_0{=}0.066\,nm, e_0 a{=}0.05538\,nm, \rho{=}2.3\,g/cm^3, \\ &L = 10r\,, p{=}0.0083\,e-6C/m^2, h{=}0.95C/m^2, \alpha_x = -1.6e-6\,K^{-1}, \eta{=}4.2 \end{aligned} \tag{51}$$

The first 10 natural frequencies of nanorods under electrical and mechanical loadings are tabulated in Tables 1 and 2 for the C–C and C–F boundary conditions, respectively. It is seen from these tables that the natural frequency for the C–C boundary condition is higher than that for the C–F boundary condition.

Table 1. The first 10 natural frequencies of nanorods for the C–C boundary condition.

Number of frequency	Natural frequency $(rad/s) \times 10^{12}$
1	1.24839
2	2.49677
3	3.74514
4	4.99348
5	6.24179
6	7.49007
7	8.73830
8	9.98648
9	11.2346
10	12.4827

Table 2. The first 10 natural frequencies of nanorods for the C–F boundary condition.

Number of frequency	Natural frequency q$(rad/s) \times 10^{12}$
1	0.624195
2	1.87258
3	3.12096
4	4.36931
5	5.61764
6	6.86594
7	8.11419
8	9.36240
9	10.6106
10	11.8586

The effect of aspect ratio (L/r) on the first natural frequency is tabulated in Tables 3 and 4 for the C–C and C–F boundary conditions, respectively. It is shown that the natural frequency decreases with increasing aspect ratios.

Table 3. The effect of aspect ratio on the first natural frequency of nanorods for the C–C boundary condition.

L/r	First natural frequency $(rad/s) \times 10^{11}$
10	12.4839
20	6.24195
30	4.16130
40	3.12098
50	2.49678
60	2.08065
70	1.78341
80	1.56049
90	1.38710
100	1.24839

Table 4. The effect of aspect ratio on the first natural frequency of nanorods for the C–F boundary condition.

L/r	First natural frequency $(rad/s) \times 10^{11}$
10	6.24195
20	3.12098
30	2.08065
40	1.56049
50	1.24839
60	1.04033
70	0.891707
80	0.780244
90	0.693550
100	0.624195

Figure 2 indicates the first natural frequency of SWBNNRs versus aspect ratio for the C–C and C–F boundary conditions and different values of nonlocal parameter (e_0a). It is seen from the results that the first natural frequency decreases with an increase in the small scale effect (e_0a) for the 2 boundary conditions, but this effect for the C–C boundary condition is higher than that for the C–F boundary condition. Moreover, the effect of small scale on the natural frequency is negligible with increasing aspect ratio of nanorods. It is shown from this figure that the natural frequency for the C–C boundary condition is higher than that for the C–F boundary condition.

Figures 3 and 4 show the small scale effect of SWBNNRs on the natural frequency with different mode numbers for the C–C and C–F boundary conditions, respectively. It can be seen from this figure that the nonlocal natural frequency $(e_0a \neq 0)$ is lower than the local natural frequency $(e_0a = 0)$. The difference between the local and nonlocal natural frequencies increases for higher natural frequencies. On the other hand, the nonlocal parameter does not have the same effect on higher mode numbers.

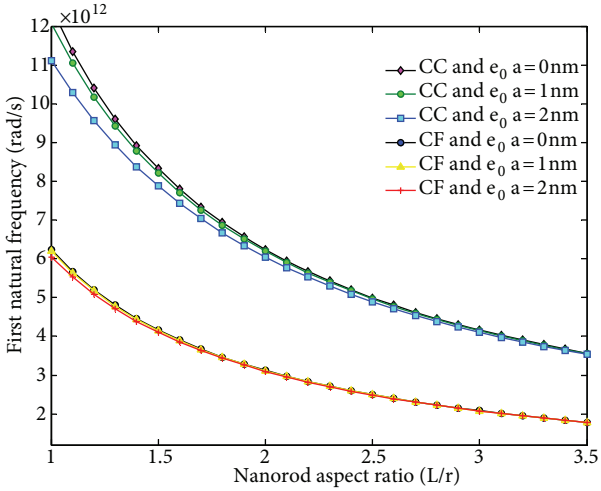

Figure 2. The effect of small scale on the first natural frequency of the nanorods for the C–C and C–F boundary conditions.

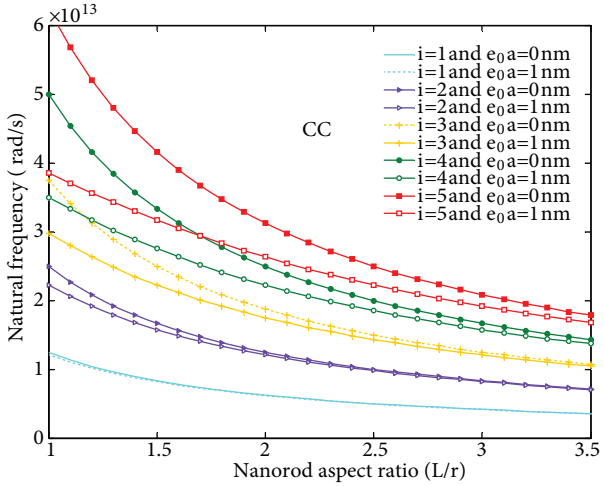

Figure 3. The effect of small scale on the first 5 natural frequencies for the C–C boundary condition.

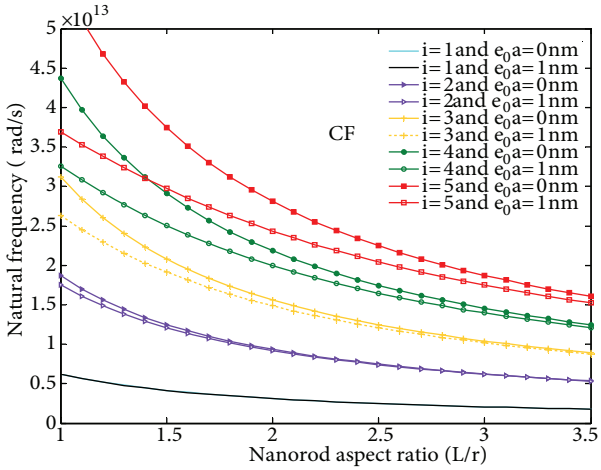

Figure 4. The effect of small scale on the first 5 natural frequencies for the C–F boundary condition.

In Figures 5 and 6, the axial displacement of SWBNNRs versus time and length of nanorods is illustrated for the C–C and C–F supported cases, respectively. It is observed from the results that Figures 5 and 6 satisfy the C–C and C–F boundary conditions.

If the electric excitation frequency is close to, but not exactly equal to, the natural frequency of SWBNNRs, the beating phenomenon occurs for the C–C and C–F boundary conditions in Figures 7 and 8, respectively.

In Figures 9 and 10, the first mode shape for different temperature changes and the 2 boundary conditions is shown. It is seen that the axial displacement of SWBNNRs increases with an increase in temperature change.

Figures 11 and 12 demonstrate the influence of the piezoelectric coefficient on the axial displacement of SWBNNRs for the C–C and C–F boundary conditions, respectively. It also can be observed that the axial displacement of SWBNNRs for both boundary conditions decreases with decreasing piezoelectric coefficient.

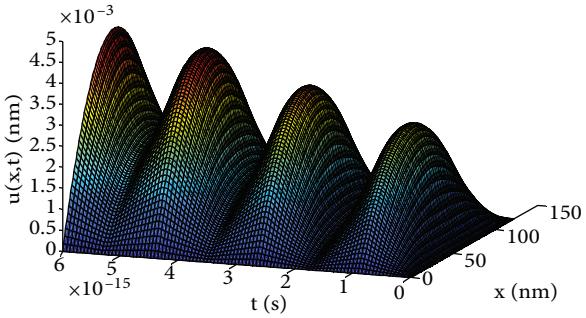

Figure 5. The axial displacement of SWBNNRs versus time and length of nanorods for the C–C boundary condition and $\Delta T = 50\,^{\circ}C$, $E_0 = 5e9\,N/nm$, $\omega' = 12e11\,rad/s$.

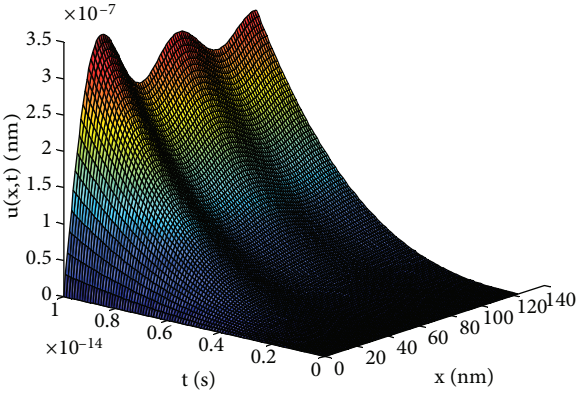

Figure 6. The axial displacement of SWBNNRs versus time and length of nanorods for the C–F boundary condition and $\Delta T = 50\,^{\circ}C$, $E_0 = 5e9\,N/nm$, $\omega' = 3e12\,rad/s$.

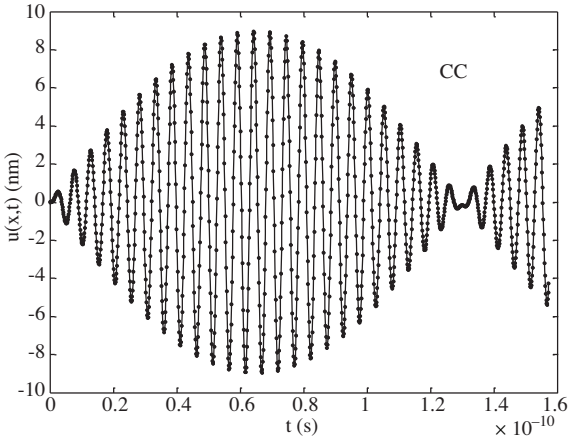

Figure 7. The axial displacement of SWBNNRs versus time for the C–C boundary condition and $\Delta T = 50\,^{\circ}C$, $E_0 = 5e9\,N/nm$, $\omega' = 1.2e12\,rad/s$, $x = 0.5L$.

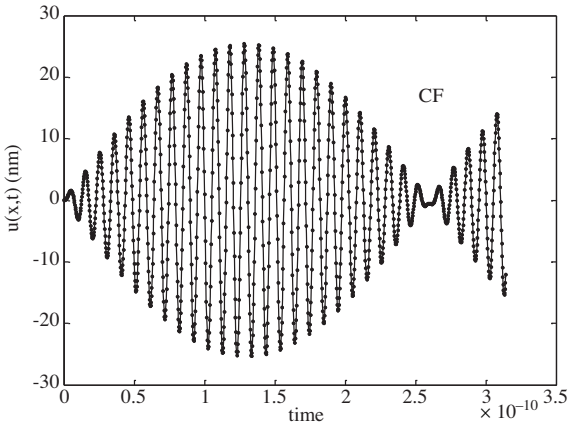

Figure 8. The axial displacement of SWBNNRs versus time for the C–F boundary condition and $\Delta T = 50^{\circ}C$, $E_0 = 5e9\,N/nm$, $\omega' = 6e11\,rad/s$, $x = L$.

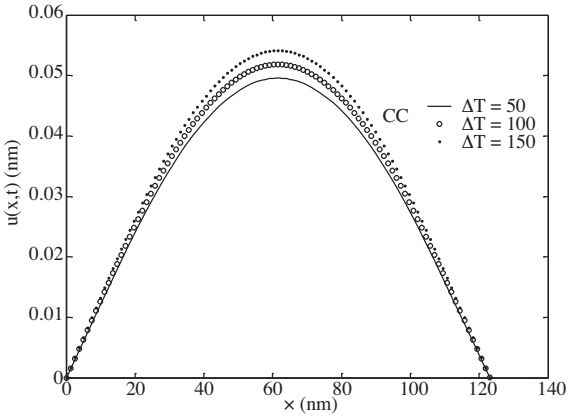

Figure 9. The influence of the temperature change on the axial displacement of SWBNNRs for the C–C boundary condition and $E_0 = 5e10\,N/nm$, $\omega' = 1.2e12\,rad/s$, $t = 3e-12\,s$.

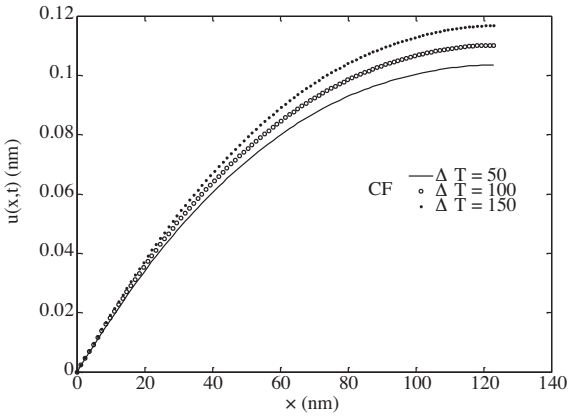

Figure 10. The influence of the temperature change on the axial displacement of SWBNNRs for the C–F boundary condition and $E_0 = 5e10\,N/nm$, $\omega' = 0.6e12\,rad/s$, $t = 3e-12\,s$.

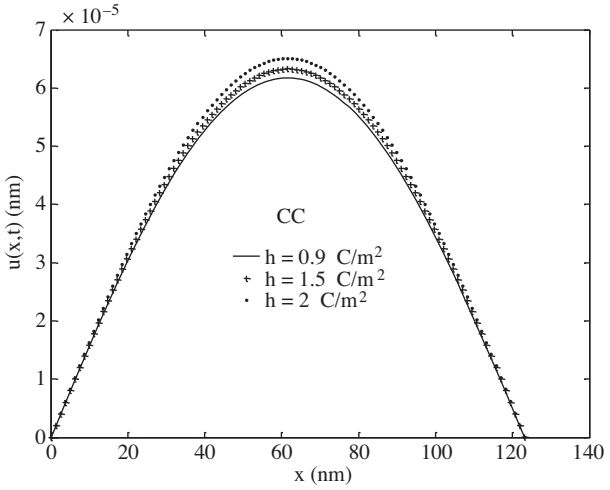

Figure 11. The influence of the piezoelectric coefficient on the axial displacement of SWBNNRs for the C–C boundary condition and $\Delta T = 50\,^{\circ}C\,, E_0 = 5e4\,N/nm\,, \omega' = 1.2e12\,rad/s,\, t = 1\,s\,.$

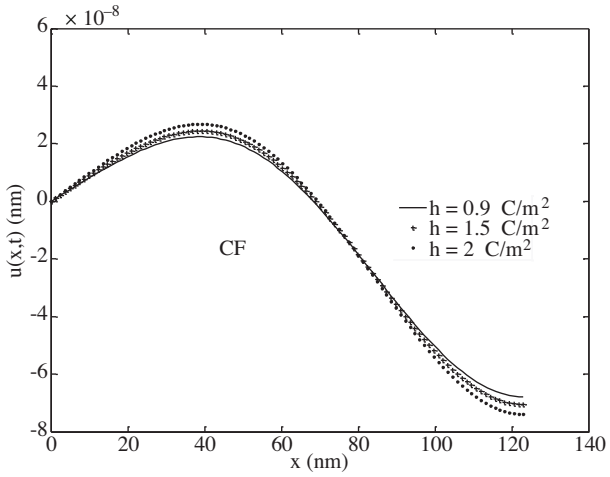

Figure 12. The influence of the piezoelectric coefficient on the axial displacement of SWBNNRs for the C–F boundary condition and $\Delta T = 50\,^{\circ}C\,, E_0 = 5e3\,N/nm\,, \omega' = 1.2e12\,rad/s,\, t = 1\,s\,.$

The influence of the dielectric constant on the axial displacement of SWBNNRs for the C–C and C–F boundary conditions is investigated as in Figures 13 and 14, respectively. It is shown from the results that an increase in the dielectric constant leads to a decrease in axial displacement.

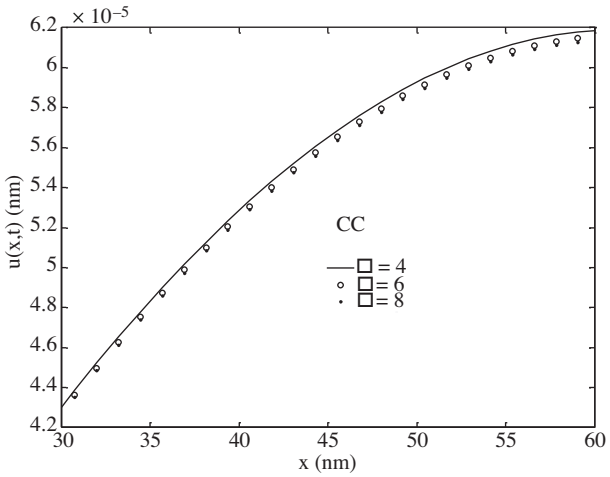

Figure 13. The influence of the dielectric constant on the axial displacement of SWBNNRs for the C–C boundary condition and $\Delta T = 50\,^{\circ}C\,, E_0 = 5e4\,N/nm\,, \omega' = 1.2e12\,rad/s,\, t = 1\,s\,.$

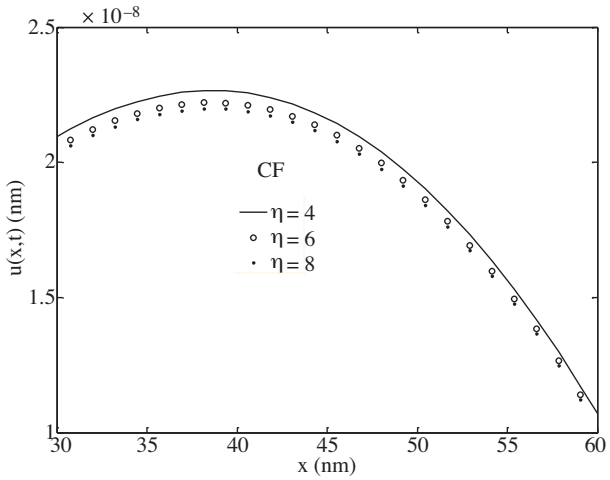

Figure 14. The influence of the dielectric constant on the axial displacement of SWBNNRs for the C–F boundary condition and $\Delta T = 50\,^{\circ}C\,, E_0 = 5e3\,N/nm\,, \omega' = 1.2e12\,rad/s,\, t = 1\,s\,.$

Figures 15 and 16 illustrate the mode shapes of SWBNNRs for the C–C and C–F boundary conditions, respectively. It is clear that different mode shapes are due to varying electric excitation frequency.

Figures 17 and 18 indicate the axial displacement versus the length of nanorods with different values of nonlocal parameter; these figures show the small scale effect on the first and fifth mode shapes for the C–C boundary condition, respectively. Comparing Figures 17 and 18 it can be concluded that the effect of small scale

on the amplitude of the axial displacement for high mode number is higher than that for low mode number. It is noted that high and low mode numbers are fifth and first mode numbers, respectively.

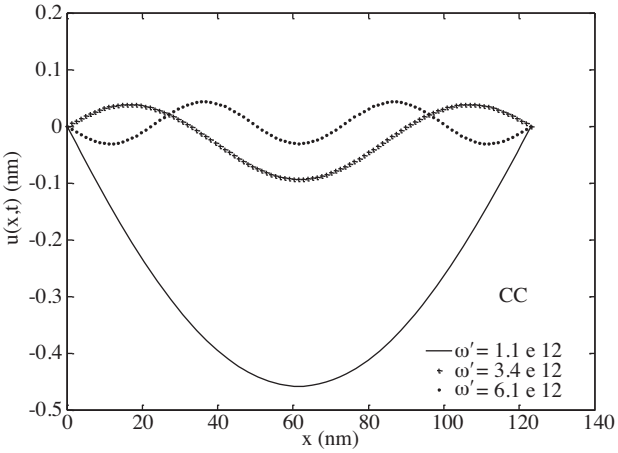

Figure 15. The mode shapes of SWBNNRs for the C-C boundary condition and $E_0 = 5N/m, \delta T = 0,\ t = 1.3e-11\ s$.

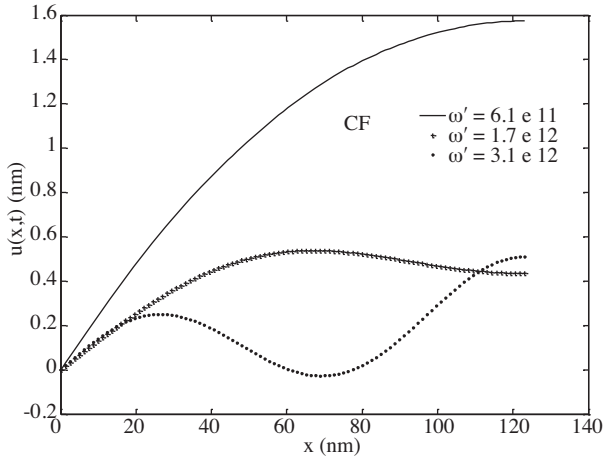

Figure 16. The mode shapes of SWBNNRs for the C–F boundary condition and $E_0 = 5\,N/nm$, $\Delta T = 0,\ t = 1.3e-11\,s$.

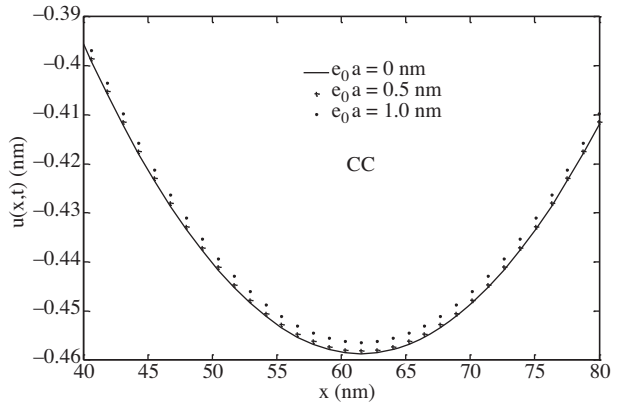

Figure 17. The effect of small scale on the axial displacement for low mode number of SWBNNRs for the C–C boundary condition and $\omega' = 1.1e12\,rad/s\,, E_0 = 5N/nm\,, \Delta T = 0\,^{\circ}C\,, t = 1\,e-11s$.

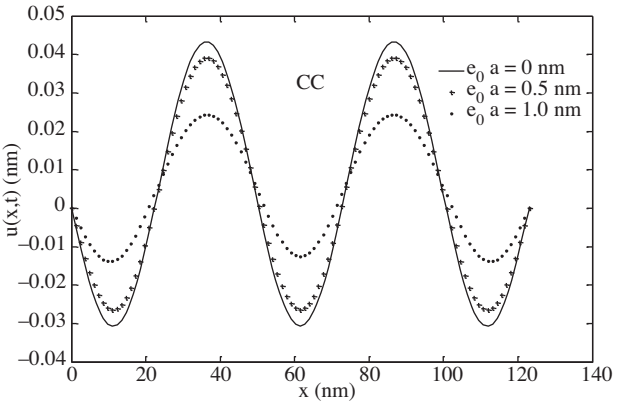

Figure 18. The effect of small scale on the axial displacement for high mode number of SWBNNRs for the C–C boundary condition and $\omega' = 6.1e12\,rad/s\,, E_0 = 5N/nm\,, \Delta T = 0\,^{\circ}C\,, t = 1\,e-11s$.

8. Conclusions

In this article, the small scale effect on the electro-thermo-mechanical vibration analysis of SWBNNRs under electric excitation is studied. The mode shapes of vibration for the C–C and C–F boundary conditions are illustrated. Moreover, the beating phenomenon is investigated for the 2 boundary conditions. The effects of the dielectric constant, piezoelectric coefficient, electric excitation, 2 boundary conditions, and temperature change on the axial displacement of SWBNNRs are presented. The following conclusions can be obtained from the present work:

1. The natural frequency decreases with an increase in the small scale effect (e_0a) or aspect ratios. On the other hand, the small scale effect is significant for lower aspect ratios and higher natural frequencies.
2. The difference between the local and nonlocal natural frequencies increases for higher natural frequencies. Moreover, the nonlocal parameter does not have the same effect on higher mode numbers.
3. The natural frequency for the C–C boundary condition is higher than that for the C–F boundary condition.
4. An increase in the axial displacement of SWBNNRs causes an increase in the temperature changes.
5. The axial displacement of SWBNNRs decreases with decreasing piezoelectric coefficient, while for the dielectric constant the results are reversed.
6. The influence of small scale on the amplitude of the axial displacement for high mode number is higher than that for low mode number.

They can be considered for nanodevices, nanoelectronics, and nanocomposites. Moreover, SWBNNRs can be used for micro- and nano-electro-thermo-mechanical devices.

Acknowledgments

The authors would like to thank the referees for their valuable comments and the Iranian Nanotechnology Development Committee for their financial support. They are also grateful to the University of Kashan for supporting this work by Grant No. 158478/1.

Nomenclature

a	an internal characteristic length
A	cross-sectional area of the nanorods
C_{ijkl}	fourth-order elasticity tensor
d	diameter of the nanorods
D	electric displacement
e_{ijk}	third-order piezoelectric tensor
e_0a	nonlocal parameter
E	Young's modulus
E_k	electric field
E_x	axial electric field
E_0	amplitude of electric excitation
G_{hi}	homogeneous solution
G_{pi}	particular solution
h	piezoelectric coefficient
h_0	thickness of the nanorods
k	thermal conduction coefficient
L	length of the nanorods
m	mass per unit length
N_x	axial force per unit length
p	pyroelectric coefficient
r	radius of the nanorods
t	time
$T(x)$	temperature change
u	axial displacement
x	longitudinal axis

Greek symbols

α_x	thermal expansion coefficient
ε_{kl}	total strain second-order tensor
ε_{kl}^{M}	mechanical strain
ε_{kl}^{T}	thermal strain
ε_x	axial strain
η	dielectric constant
ρ	density of the nanorods
σ_{ij}	stress second-order tensor
σ_x	axial stress
ω	dimensional natural frequency
ω'	frequency of electric excitation
Ω	nondimensional natural frequency
∇^2	Laplace operator

References

Aydogdu, M., "Axial Vibration Analysis of Nanorods (Carbon Nanotubes) Embedded in an Elastic Medium Using Nonlocal Elasticity", Mechanics Research Communications, 43, 34–40, 2012.

Aydogdu, M., "Axial Vibration of the Nanorods with the Nonlocal Continuum Rod Model", Physica E, 41, 861–864, 2009.

Aydoğdu, M. and Ece, M.C., "Vibration and Buckling of In-Plane Loaded Double-Walled Carbon Nano-Tubes", Turkish Journal of Engineering and Environmental Sciences, 31, 305–310, 2007.

Bansal, N.P., Hurst, J.B. and Choi, S.R., "Boron Nitride Nanotube-Reinforced Glass Composites", Journal of the American Ceramic Society, 89, 388–390, 2006.

Eringen, A.C., "On Differential Equations of Nonlocal Elasticity and Solutions of Screw Dislocation and Surface Waves", Journal of Applied Physics, 54, 4703–4710, 1983.

Fu, Y.M., Hong, J.W. and Wang, X.Q., "Analysis of Nonlinear Vibration for Embedded Carbon Nanotubes", Journal of Sound and Vibration, 296, 746–756, 2006.

Ghorbanpour Arani, A., Amir, S., Shajari, A.R. and Mozdianfard, M.R., "Electro-Thermo-Mechanical Buckling of DWBNNTs Embedded in Bundle of CNTs Using Nonlocal Piezoelasticity Cylindrical Shell Theory", Composites: Part B, 43, 195–203, 2012a.

Ghorbanpour Arani, A., Amir, S., Shajari, A.R., Mozdianfar, M.R., Khoddami Maraghi, Z. and Mohammadimehr, M., "Electro-Thermal Non-Local Vibration Analysis of Embedded DWBNNTs", Proceedings of the Institution of Mechanical Engineers, Part C: Journal of Mechanical Engineering Science, 226, 1410–1422, 2012b.

Ghorbanpour Arani, A., Mohammadimehr, M., Arefmanesh, A. and Ghasemi, A., "Transverse Vibration of Short Carbon Nanotube Using Cylindrical Shell and Beam Models", Proceedings of the Institution of Mechanical Engineers, Part C: Journal of Mechanical Engineering Science, 224, 745–756, 2010.

Ghorbanpour Arani, A., Zarei, M.S., Mohammadimehr, M., Arefmanesh, A. and Mozdianfard, M.R., "The Thermal Effect on Buckling Analysis of a DWCNT Embedded on the Pasternak Foundation", Physica E, 43, 1642–1648, 2011.

He, X.Q., Kitipornchai, S. and Liew, K.M., "Buckling Analysis of Multi-Walled Carbon Nanotubes: a Continuum Model Accounting for Van Der Waals Interaction", Journal of Mechanics of Physics and Solids, 53, 303–326, 2005.

Iijima, S., "Helical Microtubes of Graphitic Carbon", Nature, 354, 56–58, 1991.

Khoshgoftar, M.J., Ghorbanpour Arani, A. and Arefi, M., "Thermoelastic Analysis of a Thick Walled Cylinder Made of Functionally Graded Piezoelectric Material", Smart Materials and Structures, 18, 115007, 2009.

Mohammadimehr, M., Saidi, A.R., Ghorbanpour Arani, A., Arefmanesh, A. and Han, Q., "Torsional Buckling of a DWCNT Embedded on Winkler and Pasternak Foundations Using Nonlocal Theory", Journal of Mechanical Science and Technology, 24, 1289–1299, 2010a.

Mohammadimehr, M., Saidi, A.R., Ghorbanpour Arani, A., Arefmanesh, A. and Han, Q., "Buckling Analysis of Double-Walled Carbon Nanotubes Embedded in an Elastic Medium under Axial Compression Using Non-Local Timoshenko Beam Theory", Proceedings of the Institution of Mechanical Engineers, Part C: Journal of Mechanical Engineering Science, 225, 489–506, 2010b.

Mustapha, K.B. and Zhong, Z.W., "The Thermo-Mechanical Vibration of a Single-Walled Carbon Nanotube Studied Using the Bubnov–Galerkin Method", Physica E, 43, 375–381, 2010.

Salehi-Khojin, A. and Jalili, N., "Buckling of Boron Nitride Nanotube Reinforced Piezoelectric Polymeric Composites Subject to Combined Electro-Thermo-Mechanical Loadings", Composites Science and Technology, 68, 1489–1501, 2008.

Shodja, H.M. and Ghahremaninejad, A., "An FGM Coated Elastic Solid under Thermomechanical Loading: a Two Dimensional Linear Elastic Approach", Surface & Coatings Technology, 200, 4050–4064, 2006.

Yoon, J., Ru, C.Q. and Mioduchowski, A., "Vibration of an Embedded Multiwall Carbon Nanotube", Composites Science and Technology, 63, 1533–1542, 2003.